Materials Science-Poland, 33(2), 2015, pp. 356-362
http://www.materialsscience.pwr.wroc.pl/
DOI: 10.1515/msp-2015-0059

DE GRUYTER OPEN

Research on high-temperature compression and creep behavior of porous Cu–Ni–Cr alloy for molten carbonate fuel cell anodes

W. LI[1,2], J. CHEN[1,2*], H. LIANG[1], C. LI[1,2]

[1]School of Energy and Power Engineering, Changsha University of Science & Technology, Changsha, Hunan 410014, China
[2]Key Laboratory of High Efficient and Clean Utilization for Energy, Education Department of Hunan Province, Changsha University of Science & Technology, Changsha, Hunan 410014, China

The effect of porosity on high temperature compression and creep behavior of porous Cu alloy for the new molten carbonate fuel cell anodes was examined. Optical microscopy and scanning electron microscopy were used to investigate and analyze the details of the microstructure and surface deformation. Compression creep tests were utilized to evaluate the mechanical properties of the alloy at 650 °C. The compression strength, elastic modulus, and yield stress all increased with the decrease in porosity. Under the same creep stress, the materials with higher porosity exhibited inferior creep resistance and higher steady-state creep rate. The creep behavior has been classified in terms of two stages. The first stage relates to grain rearrangement which results from the destruction of large pores by the applied load. In the second stage, small pores are collapsed by a subsequent sintering process under the load. The main deformation mechanism consists in that several deformation bands generate sequentially under the perpendicular loading, and in these deformation bands the pores are deformed by flattering and collapsing sequentially. On the other hand, the shape of a pore has a severe influence on the creep resistance of the material, i.e. every increase of pore size corresponds to a decrease in creep resistance.

Keywords: *porous Cu–Ni–Cr alloy; high temperature; compression behavior; creep behavior*

1. Introduction

The molten carbonate fuel cell (MCFC) operating at approximately 923 K has been extensively studied by many investigators because of its high efficiency and possibility of utilization for a wide variety of fuels, such as coal gas and even natural gas. Anodes with sufficient structural and morphological stability are required to achieve creep resistance, but conventional nickel anodes do not meet this requirement [1, 2]. Furthermore, nickel is relatively expensive. Accordingly, cheaper anode material, which can replace nickel, has been explored. Copper has been found to be more suitable material than nickel. By the combination of high thermal conductivity and relatively high mechanical strength and toughness over a wide range of temperatures, copper alloys are likely the best materials for complex structural applications subjected to conditions of extreme heat flux under load [3]. The addition of nickel on the copper anode increases its electrochemical performance [4]. It has also been found [5] that the sintering resistance of nickel anodes can be increased remarkably by adding about 15 wt.% Cr. Therefore, in the present study, the porous Cu containing 35 wt.% Ni and 15 wt.% Cr was prepared by sintering.

Sintered materials are typically characterized by residual porosity after sintering, which is quite detrimental to the mechanical properties of these materials [6–8]. The nature of the porosity is controlled by several processing variables, such as green density, sintering temperature and time, alloying additions, and particle size of the initial powders [6]. In particular, the fraction, size, distribution, and morphology of the pores have a profound impact on the mechanical behavior [7, 9–11]. Under monotonic tensile loading, porosity reduces

*E-mail: lwzzgjajie@126.com

the effective load bearing cross-sectional area and acts as a stress concentration site for strain localization and damage, decreasing both strength and ductility. With an increase in porosity fraction (>5 %), the pores tend to be interconnected. However, the pores are relatively isolated at a porosity fraction below 5 %. In general, irregular pores have a higher stress than perfectly round pores [12, 13]. Pores have also been shown to act as linkage sites for crack propagation through interpore ligaments [7, 11]. Here, the heterogeneous nature of the microstructure plays an important role by contributing to crack tortuosity. At present, the research on the effect of pores on compression properties of porous Cu alloys has been rarely reported. Therefore, it is necessary to understand the correlation between pore structure and high temperature compression creep behavior in porous Cu alloys.

In this study, we have conducted a systematic investigation of high temperature compression experiments on porous Cu–Ni–Cr alloy matrix with 24 to 48 % porosity. The effect of pore structure on the compression properties of porous Cu alloys was studied.

2. Experiment

2.1. Preparation of porous Cu–Ni–Cr sintered alloys with different porosity

The chemical composition of porous Cu alloy powder consisted of Ni 35 wt.%, Cr 15 wt.% and the balance amount of Cu. Both the carbonyl Ni powders of an average diameter 3 to 4 μm and Cr powders with an average particle size of 5 to 8 μm were near spherical. Air atomized Cu powder, having a mean particle size of 25 to 35 μm, was used as the raw material. The porous metals were prepared by powder sintering. Carbonyl Ni powders, Cr powders and air atomized Cu powder were mixed first in a dry air condition in a high energy ball mill for 15 minutes.

Mixed powders were then blended with 3 % stearic acid as a pore forming agent and then loosely packed into a graphite mould with a diameter of 12 mm and height of 15 mm. The green samples were subsequently heated under controlled temperatures to remove the stearic acid, and finally sintered in a tube furnace in hydrogen environment to avoid oxidation. The thermogravity measurement conditions were as follows: heating rate 5 °C/min in H_2 gas atmosphere with gas flow of 50 ml/min. The final sintering processing was carried out at 300 °C for 30 min and the powder was sintered at 950 °C for 2 h with both heating and cooling rate set at 5 °C/min. Following sintering, the porosity of the sintered alloys was measured using oil-intrusion and image analysis techniques.

2.2. Compression and creep tests

A RDL05 electronic creep-fatigue testing machine was used to carry out quasi-static compression and creep tests on cylindrical samples (Φ 8 mm × 12) of various porosities. Optical microscopy and scanning electron microscopy were used to characterize the sintered porous Cu–Ni–Cr alloy.

3. Results and discussion

3.1. Microstructure

Optical microscopy reveals different microstructures for both two alloys, particularly in terms of pore size, morphology, and distribution (Fig. 1). The pores in Sample 1 appear to be much smaller and more irregular than the pores in the other alloy. It can be seen from Fig. 1(a) that these spherical pores have closed shapes, completely isolated and disconnected. Quantitative analysis of the pore size distribution of the pores with an average size of 90 to 200 μm, shown in Fig. 1a, reveals that the Sample 1 has higher density of larger pores, while Sample 2, with higher porosity (Fig. 1b), has a much larger pore size of 150 to 300 μm and higher number of connected pores. It indicates that an increase in the mean diameter of pores results in a somewhat higher number of connected pores.

3.2. Compression behavior

The compression test is the basis of the creep test. The stress-strain curves can be used to predict the level of the relative creep load. Fig. 2 shows

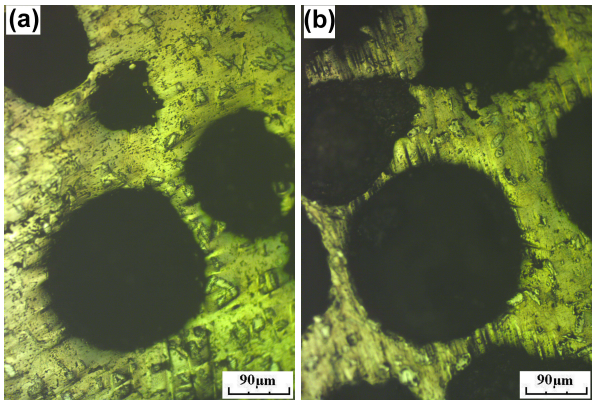

Fig. 1. Microstructure of porous Cu–Ni–C alloys with different porosities of: (a) 24.76 %; (b) 46.63 %.

the compressive stress-strain curves of porous Cu alloys with porosity of 24.76 % and 46.63 %. It is found that the curves exhibit three distinct regions (three deformation stages) under compressive loading, i.e. a linear elastic stage, an elastic stage followed by a plateau stage that occurs after yielding, and a final densification region, where the stress increases drastically. Moreover, the sample with lower porosity exhibits higher compression strength, elastic modulus and yield stress.

The behavior observed during compression deformation will be examined in order to determine the appropriate rheological law. Fig. 3 shows the failure mode during compressive deformation of the porous Cu alloy with porosity of 46.63 %. As compared to Fig. 3b, Fig. 3a shows that the linear elastic deformation tends to occur on the pore walls between adjacent holes. When the number of pores in which the generated plastic deformation, compression deformation and fracture accumulate to a certain degree, a region with small stress fluctuation is observed in Fig. 3c. With the increase of compression load, the edges of the pores in the porous Cu alloy begin to contact each other, which results in densification observed in Fig. 3d. After achieving a critical strain (∼0.4), further increase of the strain leads to the compression stress increasing linearly. There are some structural defects in the porous Cu alloy specimen, such as the pore wall rupture and wrinkling etc, which have a strong effect on the elastic modulus and mechanical properties of this material. Furthermore, pore shape and the distribution of pores also have an intense influence on the mechanical properties in this alloy.

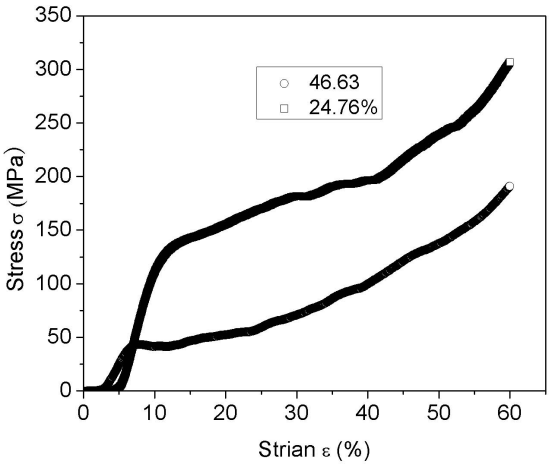

Fig. 2. Typical stress-strain curves for porous Cu–Ni–Cr alloys with different porosities at 650 °C.

3.3. Creep compression behavior

The creep compression behavior of porous Cu alloys with different porosity of 24.76 % and 46.63 % is depicted in Fig. 4. All samples show a primary creep stage at the beginning of the test followed by the stationary creep stage reaching a stationary creep rate. Obviously, the creep stress has a systematic and pronounced effect on creep behavior, as shown in Fig. 4a and 4b. Specimens subjected to a higher creep stress show higher creep strain and a faster creep strain rate. In comparison with Fig. 4b, the porous alloy with lower porosity exhibits superior creep compression resistance at the same condition, i.e. less creep strain and lower creep strain rate. Although there is much difference in the creep resistance of the two kinds of materials, their trends of creep rate are very similar, as shown in Fig. 4c and 4d. The behavior of creep rate of every sample can be divided into three stages. In the first stage, the rapid creep strain of all samples is shown within 1 h from the start. In the second stage, 1 to 10 h, creep strain increases relatively slowly. And in the final stage, the creep compressive load has a systematic and great

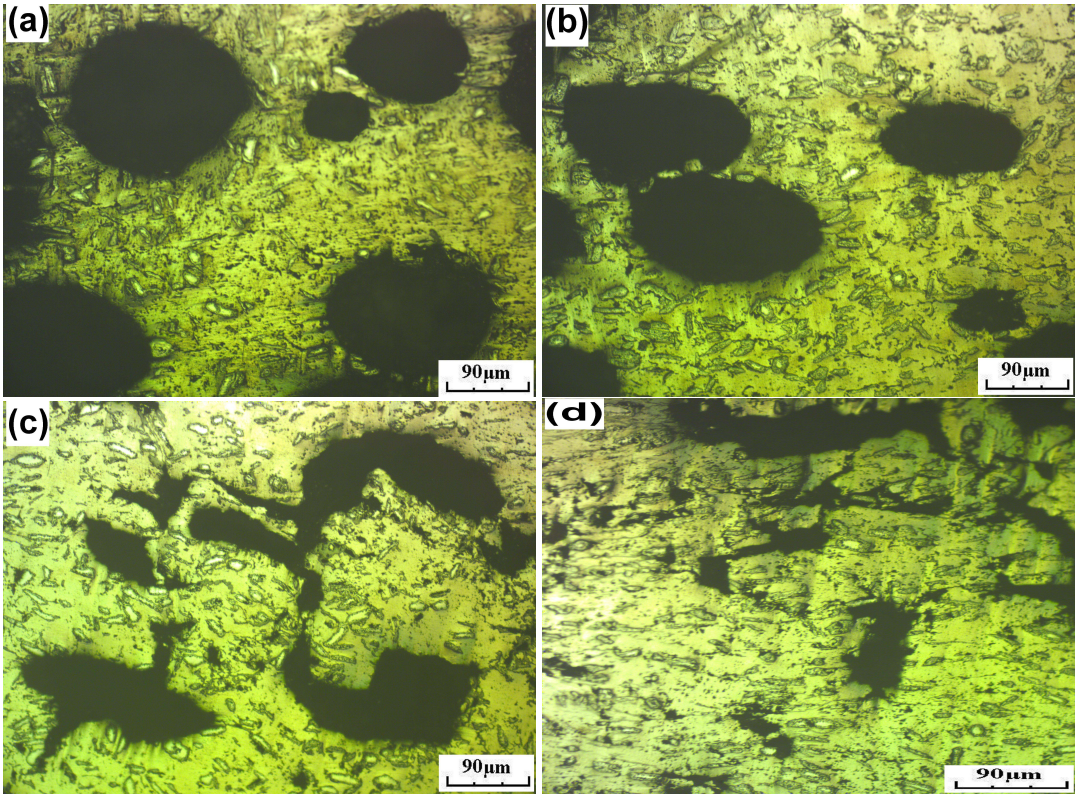

Fig. 3. Microstructure of porous Cu–Ni–Cr sintered alloy with 46.63 % porosity at different compression strains (ϵ): (a) 0; (b) 0.1; (c) 0.35; (d) 0.60.

influence on the creep behavior. Under creep stress of 20 MPa, the creep rate for the alloy with porosity of 24.67 % reaches a steady-state more quickly compared with that of sample with 46.63 % porosity. The creep strain rate for the alloy with 24.67 % porosity remains constant after about 30 h. The creep strain rate in the steady-state is 6.08×10^{-9} and 1.14×10^{-8} for the alloy with 24.76 % and 46.63 % porosity, respectively.

The $\epsilon = f(t)$ creep curve of these porous alloys exhibits two stages: a first transient one of very small duration (1 h) is followed by a fairly linear stage, corresponding to some steady-state. This is different from $\epsilon = f(t)$ creep curves observed for high density polycrystalline materials, which are generally composed of three stages. The first stage, during which (possibly after an instantaneous load) the creep rate decreases rapidly with time, is related to a change in the pore structure of the alloys. The creep rate of 46.63 % porosity sample decreases faster than the rate of the 24.76 % sample with increasing creep time; the latter shows a little change after 30 h. The creep rates of both alloys are almost time-invariant after 50 h. This period is considered as the second stage which is analogous to the steady-state creep or secondary creep of the high-density material. The dependence of stationary creep strain rate on stress is depicted in Fig. 5 for both the 24.76 % and 46.63 % porosity Cu alloys. The values obtained for the power law creep exponent n are also indicated. The corresponding Norton exponent n of the 46.63 % porosity Cu alloy becomes somewhat higher than that for the 24.76 % porosity sample. It indicates that the stationary strain rate versus stress for Cu alloy with 46.63 % porosity converges at higher stresses.

Fig. 6 shows the characteristic fracture modes during compressive creep deformation for the porous Cu alloy with porosity of 46.63 %, parallel to the creep compression direction. In compari-

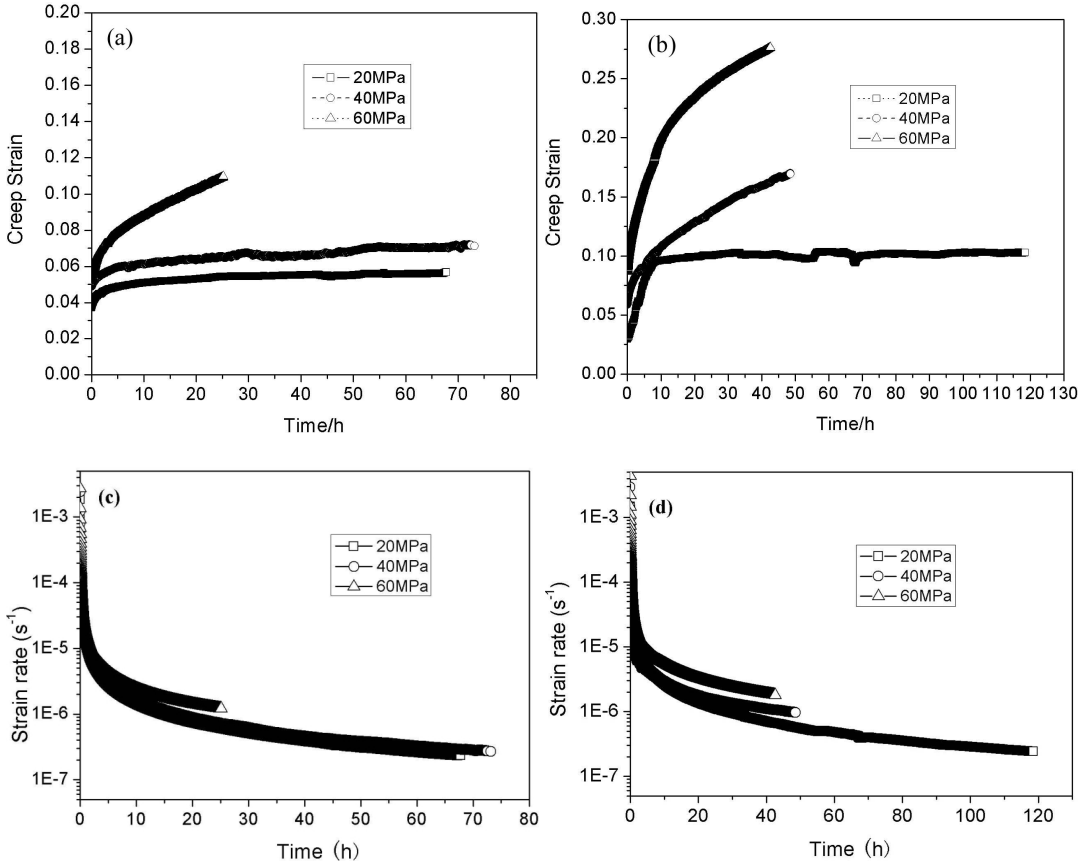

Fig. 4. Creep curves (strain/strain rate versus time) for Cu–Ni–Cr alloy with porosity of (a) and (c): 24.76%; (b) and (d): 46.63%.

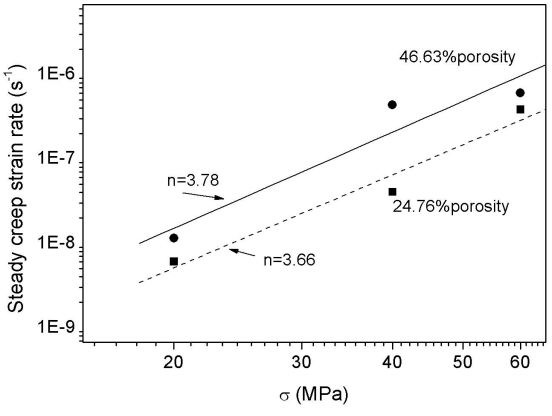

Fig. 5. Dependence of steady creep strain rate on applied stress σ obtained for the porous Cu alloys.

son with the as-received sample (Fig. 6a), the alloy fracture occurs at an angle of approximately 45° to the creep load axis, as arrowed by A in Fig. 6b. Fig. 6b also illustrates that the stress concentration tends to occur in the area located adjacent to pores. Almost all microscopic crack initiation sites are located along the pore walls, as arrowed by B, C and D in Fig. 6b. With increasing the creep time, the microscopic cracks grow and eventually coalesce to form one or more macroscopic cracks. Finally, the alloy fracture surfaces show an evidence of primary intergranular failure through a network of marcospic cracks and pores.

The surface morphologies of porous Cu with 24.76 % and 46.63 % porosity after 90 h creep test under the load of 20 MPa, perpendicular to the creep compression direction, are shown in Fig. 7. Compared to the as-received condition (Fig. 1), the samples subjected to creep stress reveal the grain rearrangement corresponding to the first stage, in which large pores are collapsed by the

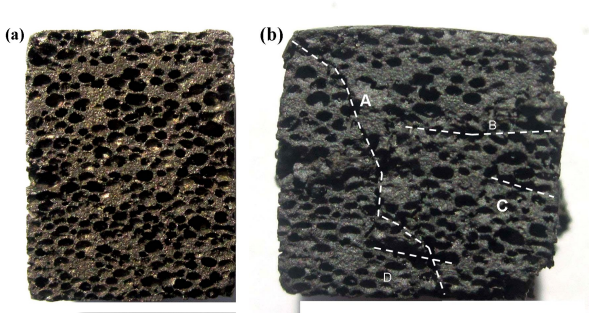

Fig. 6. Images showing creep compression failure modes for porous Cu alloy with 46.63 % porosity, parallel to the creep compression direction, (a) as-received sample; (b) sample after 90 h creep test (650 °C/20 MPa).

rearrangement of the grains to stable sites due to the compressive stress and the bending moment exerted in the vicinity of the neck; large pores are virtually destroyed during this stage. In the second stage, small pores are diminished by the sintering stress due to mass transport accelerated under applied stresses. For the 24.76 % and 46.63 % porosity samples, no grain growth is observed in the surface. Creep deformation in the two alloys results from deformation of the pore structure by the load rather than by sintering. For the larger porosity sample, most of the large pores are rapidly collapsed by grain rearrangement during 10 h, and the deformation continues during the second stage, as shown in Fig. 6. The porosity is decreased to 30 % after 90 h of the creep test and the pore structure is considerably collapsed. On the other hand, the creep behavior of 24.76 % porosity sample is restricted to the first stage, and the deformation is mainly caused by the applied load rather than sintering shrinkage. Therefore, the enhanced creep compression behavior of the denser alloys could be attributed to smaller pore size and porosity which results in more homogeneous deformation and decreased strain localization in the material.

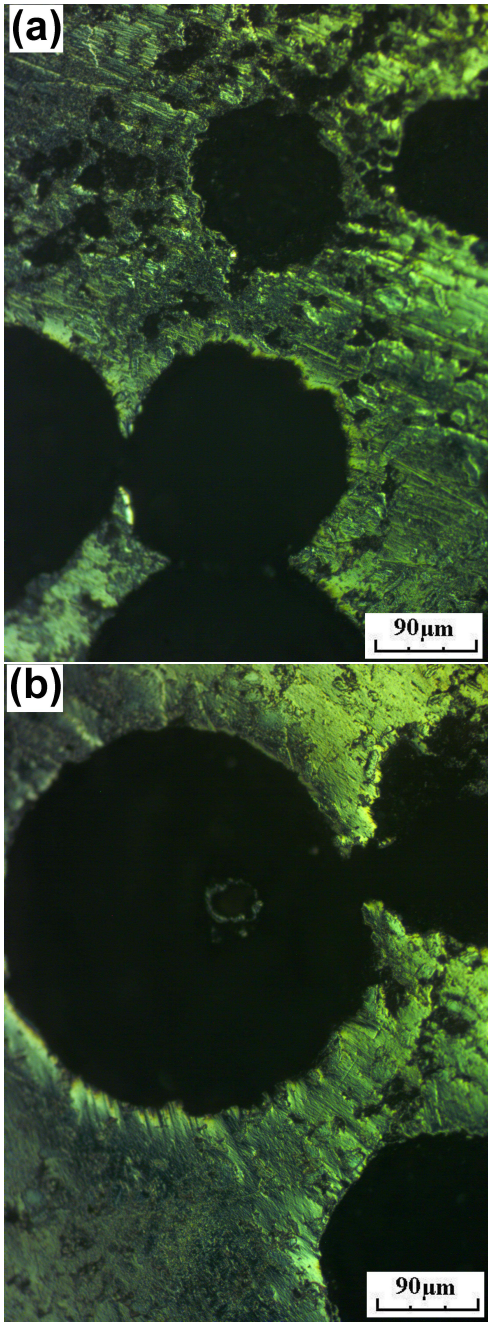

Fig. 7. SEM images of porous Cu–Ni–Cr after 90 h creep test (650 °C/20 MPa) perpendicular to the creep compression direction (a) with 24.76 % porosity and (b)with 46.63 % porosity.

4. Conclusions

1. The compression strength, elastic modulus, yield stress of the investigated samples increased with a decrease in Cu alloy porosity. The compression deformation process has been classified in terms of three stages of linear elastic deformation, yielding plateau area with pore wall buckling, collapse, and plastic deformation with pore densification.

2. The enhanced compression behavior of the denser alloys can be attributed to smaller pore size and reduced porosity which results in more homogeneous deformation and decreased strain localization in the material.
3. The creep compression resistance increases with a decrease in Cu porosity. The first stage relates to grain rearrangement which results from the destruction of large pores by the applied load. In the second stage, small pores are collapsed by a subsequent sintering process under the load.

Acknowledgements

The authors are grateful to the National Natural Science Foundation of China (51075044, 51471036), Energy efficient and clean use of open fund of Key Laboratory of Colleges and Universities in Hunan Province (12K079).

References

[1] LEE H., LEE I., LEE D., *J. Power Sources*, 162 (2006), 1088.
[2] SWAH K.H.W., HAMPURAN T.R., CHEN X., *Corros. Sci.*, 37 (1995), 1333.
[3] LI G., THOMAS B.G., STUBBINS J.F., *Metall. Mater. Trans.*, 31 (2000), 31, 2491.
[4] KIM Y.S., LEE K.Y., CHUN H.S., *J. Power Sources*, 99 (2001), 26.
[5] MARIANOWSKI L.G., DONADO R.A., MARU H.C., *US Patent No. 427476004* (27 Jan, 1981).
[6] KIM D., LEE I., LIM H., *J. Power Sources*, 109 (2002), 347.
[7] POLASIK S.J., WILLIAMS J.J., CHAWLA N., *Metall. Mater. Trans. A*, 33 (2002), 73.
[8] INSU J., TADASHI A., *Acta Mater.*, 53 (2005), 3415.
[9] CHAWLA N., MURPHY T.F., NARASIMHAN K.S., *Mat. Sci. Eng. A-Struct.*, 308 (2001), 180.
[10] LIU X.J., HUAI Z., LU Y., *Mat. Sci. Eng. A-Struct.*, 545 (2012), 111.
[11] CHAWLA N., JESTER B., VONK D., *Mat. Sci. Eng. A-Struct.*, 346 (2003), 266.
[12] SEN D., MAHATA T., PATRA A.K., MAZUMDER S., SHARMA B., *Pramana-J. Phys.*, 63 (2004), 309.
[13] CHAWLA N., DENG X., *Mat. Sci. Eng. A-Struct.*, 390 (2005), 98.

Received 2014-09-24
Accepted 2015-03-17